Protoplasma (2016) 253:787–802
DOI 10.1007/s00709-015-0833-2

ORIGINAL ARTICLE

Comparison of cell death and accumulation of reactive oxygen species in wheat lines with or without *Yr36* responding to *Puccinia striiformis* f. sp. *tritici* under low and high temperatures at seedling and adult-plant stages

Hui Li[1] · **Bin Ren**[1] · **Zhensheng Kang**[1] · **Lili Huang**[1]

Received: 18 December 2014 / Accepted: 12 May 2015 / Published online: 13 June 2015

Abstract *Yr36* is an important gene conferring resistance to stripe rust of wheat caused by *Puccinia striiformis* f. sp. *tritici* (*Pst*). To determine if the *Yr36* resistance is correlated to reactive oxygen species (ROS) burst and cell death, wheat near-isogenic lines with (UC1041+*Yr36*) and without (UC1041) the gene were histologically characterized for response to *Pst* infection. *Yr36* conferred stripe rust resistance at both seedling and adult-plant stages when the gene line was tested with *Pst* race CYR29 at a high-temperature (HT) cycle (12 °C at night and 33 °C during the day). At the HT cycle, the growth of secondary hyphae was obviously suppressed in both seedlings and adult plants of UC1041+*Yr36* compared with those of UC1041. The percentages of infection sites with necrotic host cells in UC1041+*Yr36* were significantly higher than UC1041 60 hours after inoculation (hai) at both seedling and adult-plant stages. Mesophyll cell death in the inoculated UC1041+*Yr36* leaves at the HT cycle was stronger than at a low-temperature (LT) cycle (12 °C at night and 18 °C during the day). At the HT cycle, the level of ROS burst started increasing in the inoculated leaves of UC1041+*Yr36* when *Pst* hyphae started differentiating and extending, and simultaneously, the number of penetration sites with hypersensitive cell death was also increasing. The results indicate that *Yr36* product affects the ROS accumulation and cell death of the host in interaction of wheat with *Pst*.

Keywords *Triticum aestivum* · *Puccinia striiformis* · Hypersensitive response · Reactive oxygen species · Plant disease resistance

Handling Editor: Peter Nick

Electronic supplementary material The online version of this article (doi:10.1007/s00709-015-0833-2) contains supplementary material, which is available to authorized users.

✉ Lili Huang
huanglili1@hotmail.com

[1] State Key Laboratory of Crop Stress Biology for Arid Areas and College of Plant Protection, Northwest A&F University, Yangling, Shaanxi 712100, People's Republic of China

Introduction

Wheat stripe rust, caused by *Puccinia striiformis* f. sp. *tritici* (*Pst*), is one of the most important diseases of wheat in the world (Chen 2005; Wellings 2011). The disease is especially important in China as it affects millions of hectares of wheat and causes huge yield losses in an epidemic year (Wan et al. 2004).

Growing resistant cultivars is the most effective and environmentally friendly method for the control of stripe rust (Chen et al. 2002; Dodds and Rathjen 2010). Most permanently named *Yr* genes confer race-specific seedling resistance (also known as all-stage resistance), and some confer nonrace-specific adult-plant resistance (Chen 2005, 2013; Lin and Chen 2007, 2009). Race-specific resistance is often not durable because the emergence of new virulent races in the pathogen population may circumvent the resistance. In contrast, nonrace-specific resistance is durable (Qayoum and Line 1985; Chen and Line 1995a, b; Line and Chen 1995; Line 2002; Chen 2005, 2013). This type of resistance is especially valuable in breeding programs to develop cultivars with durable resistance.

High-temperature adult-plant (HTAP) resistance is usually effective after stem elongation and more durable than seedling resistance (Qayoum and Line 1985; Milus and Line 1986a, b; Line and Chen 1995). Some cultivars with HTAP resistance have remained resistant for more than 40 years in the US

Pacific Northwest, even when they have been grown extensively and exposed to numerous races of the pathogen (Line and Chen 1995; Chen 2005, 2013). *Yr36* was originally considered as an HTAP resistance gene (Uauy et al. 2005). However, the gene is more temperature sensitive and less growth-stage dependent, because it has been shown to provide different levels of resistance at different growth stages when exposed to temperatures over 25 °C (Fu et al. 2009). Segovia et al. (2014) reported that the adult plants of a wheat line with *Yr36* showed partial resistance below 18 °C. These studies demonstrate that *Yr36* can provide resistance at a wide range of temperatures although the resistance level varies, which is a characteristic of durable resistance. So far, *Yr36* has not been found to be race specific although it is less or not effective when plants are at seedling stages and/or at low temperatures (Uauy et al. 2005). Thus, the gene is valuable for breeding wheat cultivars with durable and adequate resistance when combined with other resistance genes. Although the gene has been cloned (Fu et al. 2009), its resistance mechanism is still not fully understood.

Rapid and transient production of reactive oxygen species (ROS), termed "oxidative burst," is one of the earliest defense reactions activated in plants in response to pathogen attack and is a hallmark of successful recognition of plant pathogens (Lamb and Dixon 1997; Torres et al. 2006; Liu and Lin 2014). ROS production is detected invariably during the activation of pathogen-induced molecular pattern-triggered immunity and effector-triggered immunity (Torres 2010). Oxidative burst is not only involved in direct antimicrobial activities, but could also be the cellular signal activating further plant defense reactions, including the induction of defense gene expression and hypersensitive response (HR) of infected cells (Tenhaken et al. 1995; Lamb and Dixon 1997; Thordal-Christensen et al. 1997; Bolwell et al. 2001). The ROS-induced HR can act as a defense reaction against avirulent pathogen isolates (Delledonne et al 1998; Hückelhoven et al. 1999). The tissue necrosis caused by ROS during pathogen infection increases host resistance to a biotrophic pathogen and, thus, could be involved in the interactions between wheat and *Pst*.

Previous histological studies on the interactions between wheat and *Pst* mostly focused on seedling resistance. The delay of hyphal differentiation and colony formation and occurrence of host cell necrosis were observed in incompatible interactions at seedling stage (Kang et al. 2003). HR and ROS were also observed in incompatible reactions of the pathosystem at seedling stage (Wang et al. 2007). *Yr1* and *Yr5* race-specific seedling resistance reactions were found to be similarly associated with a rapid cell death response and early retardation of *Pst* infection (Coram et al. 2008; Bozkurt et al. 2010). Among few studies on adult-plant resistance (APR), Zhang et al. (2012) found that HR and ROS burst were involved in the APR of wheat genotype XZ 9104 against stripe rust. However, the *Lr34*/*Yr18* and *Lr46*/*Yr29* loci conferring APR to both leaf rust and stripe rust are not associated with significant HR in the host (Singh 1992; Rubiales and Niks 1995; William et al. 2003). These studies indicate that the responses conferred by different resistance genes to stripe rust can be different.

In order to determine if ROS burst and cell death are related to *Yr36*-conferring resistance to stripe rust, we conducted a histological study. We focused the study on (1) *Pst* development and hypersensitive reaction of the host cells in wheat plants with *Yr36* and (2) *Pst*-triggered ROS accumulation in host cells during the interaction between the wheat plants with *Yr36* and the rust fungal pathogen.

Materials and methods

Plants and pathogens

Hexaploid spring wheat (*Triticum aestivum* L.) near-isogenic lines UC1041 and UC1041+*Yr36* were used in this study. Both lines were developed by the University of California, Davis (Uauy et al. 2005; Fu et al. 2009), and the seeds of these lines were provided by Dr. Daolin Fu in Shandong Agricultural University, Tai'an, China.

The wheat cultivar Avocet Susceptible (AvS) was used as a susceptible control to ensure the success of inoculation in the experiments. To choose a *Pst* race virulent on UC1041 at both seedling and adult-plant stages, Chinese *Pst* races CYR25, CYR29, CYR32, and CYR33, as described by Chen et al. (2009), were tested. The urediniospores of these races were from the *Pst* collection kept in our stripe rust program in the College of Plant Protection, Northwest A&F University.

Inoculation and recording of infection types

Wheat lines UC1041 and UC1041+*Yr36*, together with susceptible control AvS, were evaluated for reactions to *Pst* in both seedling and adult-plant stages.

For the seedling test, about 20 seeds were planted in a clay pot (10 cm at the top and 5 cm at the bottom in diameter with 6 cm in height) filled with a soil mixture. For the adult-plant test, after vernalization of germinated seeds for 4 weeks at 4 °C, wheat seedlings were transplanted into pots of 20 cm in diameter filled with a soil mixture to produce adult plants.

Fresh urediniospores were applied with a paintbrush onto the surface of wheat leaves. The entire surface of each leaf was uniformly brushed with urediniospores. Inoculations were carried out separately on flag leaves of wheat at the boot stage (adult-plant stage) and on the second leaves of wheat at the seedling stage. The inoculated plants were placed in a dew chamber without light at 10 °C for 24 h and then divided into two groups. One group was grown in a greenhouse at a low-temperature (LT) cycle (12 °C at night and 18 °C during the

day), and another group was grown at a high-temperature (HT) cycle (12 °C at night and 33 °C during the day). Both greenhouses were set with the same photoperiod cycle (16 h light, 60 μmol/m^2/s photon flux density/8 h dark) with the higher temperature in each cycle during the photoperiod. The infection type (IT) data of seedlings and adult plants were recorded based on a 0–9 scale (Line and Qayoum 1992) 14 and 21 days after inoculation (dai).

Histopathological analysis of the wheat-*Pst* interactions

In order to observe histopathological changes during the infection process, inoculated leaves were harvested 18, 24, 36, 48, 60, 72, 96, 120, 144 and 168 hours after inoculation (hai), of which 18 and 24 hai were in the dark period and all of the others were in the light period. Then, 1.5 cm leaf segments cut from the center of inoculated leaves were fixed and decolorized in an ethanol/trichloromethane (3:1, *v*/*v*) solution containing 0.15 % (*w*/*v*) trichloroacetic acid for at least 48 h. The leaf samples were cleared in saturated chloral hydrate until leaf tissues were translucent. To visualize *Pst* structures, the leaves were stained with calcofluor (Sigma-Aldrich, St. Louis, MO, USA) as described by Kang et al. (1993). All calcofluor-stained tissues were examined under a fluorescence microscope using 485 nm excitation filter, 510 nm dichromic mirror, and 520 nm barrier filter.

For each wheat sample, 30–50 infection sites from 8 to 10 leaf segments of three leaves were examined for colony length and area of attacked mesophyll cells. Presence of a substomatal vesicle was defined as an established penetration site. The maximum linear length of the fungal colonies parallel to the length of the leaf was measured. Plant cell death was defined by the presence of autofluorescence associated with an infection unit under a fluorescent microscope (exCitation filter 485 nm, dichromic mirror 510 nm, barrier filter 520 nm) or plasmolysis detected using a differential interference microscope. The number of penetration sites showing plant cell death was converted to the percentage of the total number of penetration sites. All microscopic examinations were done with an Olympus BX-51 microscope (Olympus Corporation, Japan). Means of linear length of the fungal colonies were compared among treatments using Duncan's multiple range test at P=0.05 of the SAS software package (SAS Institute, Cary, NC). The same analysis was done to determine the area of necrotic mesophyll cells.

Detection of H_2O_2 and O_2^- (ROS)

The generation of H_2O_2 during the wheat-*Pst* interactions was analyzed histochemically using the 3,3-diaminobenzidine (DAB; Amresco, Solon, OH, USA) staining method as described by Thordal-Christensen et al. (1997). The detection of O_2^- was carried out using the nitroblue tetrazolium (NBT, Amresco, Solon, OH, USA) staining according to the procedure described by Doke (1983) and Wang et al. (2007). Leaf samples were harvested at the same time as those for the histopathological analysis. The leaf samples were fixed and decolorized before microscopic examinations as described above. The appearance of brownish and blue colors in leaf tissue indicated the presence of H_2O_2 and O_2^-, respectively. The number of penetration sites showing DAB or NBT staining was converted to the percentage of the total number of penetration sites.

Results

Selection of *Pst* race CYR29 for characterization of the *Yr36* resistance

The seedlings of both UC1041 and UC1041+*Yr36* were resistant to CYR25 and CYR33 at the LT cycle, but moderately susceptible (IT>4) to CYR29 and CYR32 at the LT cycle (Online Resource 1). Based on these data, CYR29 and CYR32 were used for the adult-plant tests. In the adult-plant and LT tests, UC1041 and UC1041+*Yr36* had similar resistant reactions when tested with CYR32 (IT<2), but had moderately susceptible reactions when tested with CYR29 (Online Resource 2). For comparison, AvS was susceptible (IT 7–8) in all of the tests. Therefore, CYR29 was selected for the further experiments to histologically characterize the interactions of the wheat lines with *Pst*.

When tested with CYR29, the seedlings of UC1041+*Yr36* had a moderately resistant reaction (IT 4–5), but those of UC1041 had a moderately susceptible reaction (IT 6–7) at the LT cycle (Fig. 1a). At the HT cycle, seedlings of UC1041+*Yr36* was highly resistant (IT 2–3), whereas UC1041 was moderately resistant (IT 4–5) (Fig. 1a). Adult plants of UC1041+*Yr36* and UC1041 had similar reactions (IT 4–5) at the LT cycle (Fig. 1b). In the HT test, adult plants of UC1041 had a moderately resistant reaction (IT 4–5), whereas adult plants of UC1041+*Yr36* had a much higher level of resistance (IT 2–3) than that in the LT test (Fig. 1b). In contrast, susceptible control AvS was susceptible (IT 7–8) in all four-way tests (Fig. 1a, b). The results showed that when characterized by IT, both UC1041 and UC1041+*Yr36* had some levels of resistance to stripe rust. The resistance in UC1041 was increased by temperature at seedling stage, and the resistance was maintained at similar levels at the adult-plant stage at both the LT and HT cycles. Compared to UC1041, the higher level of resistance in UC1041+*Yr36* was attributed to *Yr36*, and the *Yr36* resistance is more sensitive to temperature. Nevertheless, *Yr36* provides its highest level of resistance at the adult-plant stage and at high temperatures. In addition, the adult plants of UC1041 became

senescent, while those of UC1041+*Yr36* remained green 30 dai (Fig. 1c).

Pst development in plant tissue

The typical early infection was observed as followings: When a urediniospore adheres to a leaf surface, it germinates and produces a germ tube. The germ tube enters a stoma, reaches the substomatal chamber, and expands to form a substomatal vesicle (SV) in the substomatal cavity. From this vesicle, one or more primary infection hyphae grow until they contact a host mesophyll cell whereupon they differentiate to form haustorial mother cells (HMCs). Subsequently, a HMC grows through the plant cell wall through invaginating the host plasma membrane as it expands and differentiates into a haustorium. The presence of an SV was considered as the establishment of a penetration site. The number of penetration sites was counted for each treatment and used to compare *Pst* infection and development among wheat lines tested at different growth stages and at different temperature cycles.

At both seedling and adult-plant stages, *Pst* SVs were formed, and primary infection hyphae were differentiated in the leaves of UC1041+*Yr36* and UC1041 at 12 hai (Fig. 2a, b). By 18 hai, most of the SVs were differentiated into primary infection hyphae and HMCs (Fig. 2c, d).

The primary infection hyphae expanded for the further differentiation at 36 hai (Fig. 3a, b), and at the meantime, hypersensitive cell death was observed in seedling leaves of

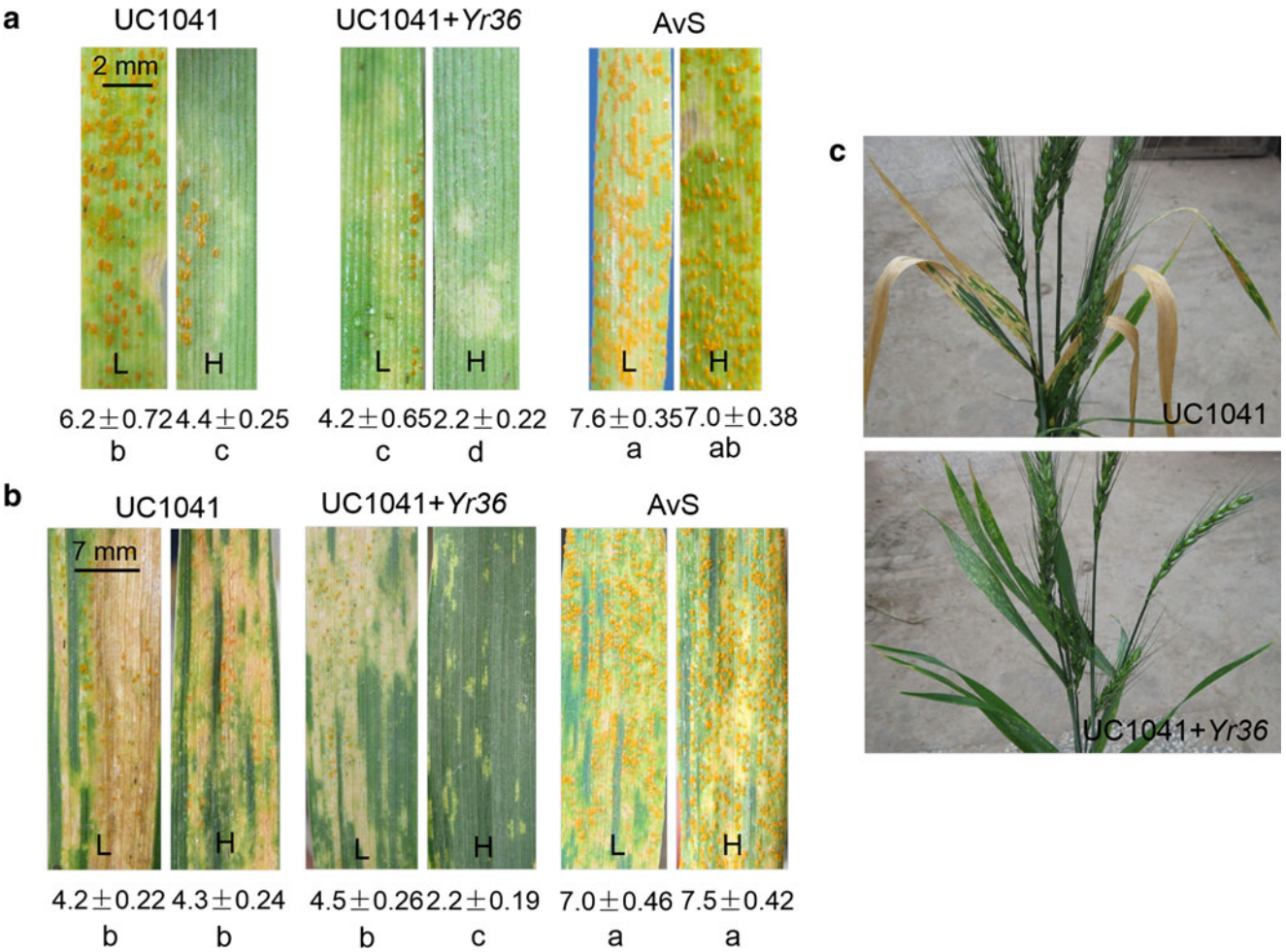

Fig. 1 Responses of seedlings and adult plants of wheat lines UC1041 and UC1041+*Yr36* inoculated with *Puccinia striiformis* f. sp. *tritici* (*Pst*) race CYR29 grown under different temperature conditions. **a** Responses of seedlings of wheat lines inoculated with *Pst*. **b** Responses of adult plants of wheat lines inoculated with *Pst*; *L* represents the low-temperature tests, 12/18 °C; *H* represents the high-temperature tests, 12/33 °C. For the temperature treatments, 12/18 °C means that plants were kept in a controlled greenhouse at 16 h light/8 h dark cycle and temperatures at 12 °C during the dark period and 18 °C during the light period; 12/33 °C means that temperature regime had a gradual change between a minimum of 12 °C at the middle of the dark period to a maximum of 33 °C at the middle of the light period. **c** Response in the adult plants of wheat UC1041 and UC1041+*Yr36* inoculated with *Pst* CYR29 under the high-temperature cycle 30 days after inoculation. Infection types of leaves were observed in the seedlings and adult plants at 14 and 21 days after inoculation, respectively. Values are means of 15 plants±standard errors of the infection types. *Means with the same letter* are not significantly different at $P=0.05$ according to Duncan's multiple range test. The wheat cultivar Avocet Susceptible (AvS) was used as a susceptible control

UC1041+*Yr36* but not in UC1041 (Fig. 3a–d). Secondary hyphae (SH) were extended (Fig. 3e–h) and observed in most penetration sites of each seedling treatment 60 hai. SH continued growing and strong hypersensitive cell death occurred in the UC1041+*Yr36* plants tested at the HT cycle 120 hai (Fig. 3i–l). Fungal colonies were observed at almost all penetration sites 144 and 168 hai. In the meantime, the expansion of fungal colonies was intense.

In the adult-plant leaves of UC1041+*Yr36* and UC1041, primary hyphae differentiated into SH at penetration site 36 hai (Fig. 4a–d), SH became contacting with host mesophyll cells, and HR appeared in UC1041+*Yr36* (Fig. 4c, d). SH continued growing as observed at 60 hai (Fig. 4e–h). By 120 hai, the percentages of penetration sites with SH in all treatments were more than 80 %, and fungal colonies were completely surrounded by necrotic mesophyll cells in some penetration sites of UC1041+*Yr36* at the HT cycle (Fig. 4i–l). Fungal colonies were intensively extended at 144 and 168 hai.

The maximum linear length of the fungal colonies parallel to the length of the leaf was measured at 60 and 120 hai at both seedling and adult-plant stages. Linear length was not measured after 120 hai because *Pst* colonies in the heavily infected leaves became overlapping and no reliable measurement could be made. The mean linear length of colonies on seedling leaves of UC1041+*Yr36* in the HT test was significantly lower than that in the LT test at 60 hai. Although the value of the UC1041+*Yr36* seedlings in the HT test was lower than that in the LT test at 120 hai, the difference was not statistically significant (Fig. 5a). At the adult-plant stage, the mean linear lengths of colonies of UC1041+*Yr36* in the HT test were significantly lower than those in the LT test at 60 and 120 hai (Fig. 5b). In the plants of UC1041+*Yr36*, colony growth was significantly reduced in the HT test.

Yr36 promotes the death of attacked mesophyll cells

In the seedling tests with CYR29, hypersensitive cell death was observed earlier in the UC1041+*Yr36* plants than in the UC1041 plants, and the percentage of penetration sites with cell death started increasing from 48 hai (Fig. 6a). From 60 hai, the percentage of penetration sites with cell death in the UC1041+*Yr36* leaves was significantly higher than that of UC1041 (Fig. 6a). Under the different temperatures, the percentage of penetration sites with dead cells in UC1041+*Yr36* was higher in the HT tests than that of the LT test at both 60 and 72 hai; however, from 96 hai, the percentages of penetration sites with dead cells in the UC1041+*Yr36* plants at HT and LT were similar (Fig. 6a). Cell death was observed in almost all penetration sites of UC1041+*Yr36* at 144 and 168 hai, and the percentage was significantly higher than that of UC1041 (Fig. 6a). However, only few penetration sites were observed with hypersensitive cell death before 96 hai in the UC1041 leaves, and the percentage of penetration sites with dead cells was increased slightly at 120 and 144 hai (Fig. 6a).

In the adult-plant tests with CYR29, cell death was observed at some penetration sites in the UC1041+*Yr36* leaves at 36 hai (Fig. 6b), whereas in the UC1041 plants, cell death was not observed until 48 hai (Fig. 6b). The percentage of penetration sites with hypersensitive cell death of UC1041+*Yr36* at HT was higher than those of the other adult-plant treatments at all tested time points (Fig. 6b). The percentage of penetration sites with hypersensitive cell death was increased rapidly after 48 hai (Fig. 6b). In the UC1041 plants, the percentages of penetration site with hypersensitive cell death were low at 18–96 hai (Fig. 6b), but increased sharply at 120 hai (Fig. 6b).

The area of *Pst*-triggered mesophyll cell death was measured at 60, 120, 144, and 168 hai. In the seedling tests, the value of UC1041+*Yr36* was significantly higher than those of the other seedling treatments at HT at 60, 144, and 168 hai,

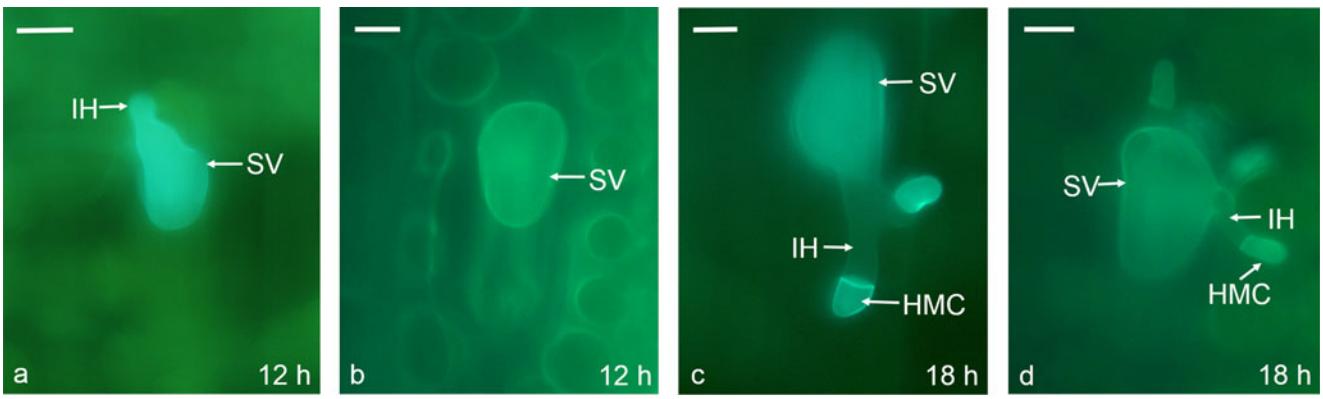

Fig. 2 Development of *Puccinia striiformis* f. sp. *tritici* seedling (**a**, **c**) and adult-plant (**b**, **d**) leaves of wheat lines UC1041 and UC1041+*Yr36* at 12 and 18 hours after inoculation (hai). **a**, **b** A germ tube grows to form SV at 12 hai; **c**, **d** SV differentiates into primary infection hyphae (*IH*) and haustorial mother cell (*HMC*). *Bars*=10 μm. *SV* substomatal vesicle, *IH* infection hypha, *HMC* haustorial mother cell

except for the insignificant differences at 120 hai (Fig. 7a). In the adult-plant tests, the area of cell death in the UC1041+*Yr36* plants tested at HT was significantly higher than the other adult-plant treatments at the measured time points (Fig. 7b). By 144 hai, the area of cell death of UC1041+*Yr36* at HT was 48,871 μm^2, which was 11 and 10 times as large as the size in the UC1041+*Yr36* leaves tested at LT and in the UC1041 leaves at HT, respectively (Fig. 7b). The area of cell death of UC1041+*Yr36* at HT was 116,840 μm^2 at 168 hai, 2 and 4 times of the values of UC1041+*Yr36* at LT and UC1041 at HT, respectively (Fig. 7b). Thus, *Yr36* promoted the death of attacked mesophyll cells at HT.

H_2O_2 accumulation in host cells

At the early penetration stage, the H_2O_2 accumulation was induced in the guard cells in contact with a germ tube or penetrated by the fungus, which was indicated by reddish-brown staining due to DAB polymerization (Fig. 8a, b). In contrast, at the postpenetration stage, differences in generation and accumulation of H_2O_2 became obvious in mesophyll cells or the cell walls of the plants at different stages infected by *Pst* (Fig. 8c, d).

At the early infection stage, no difference in H_2O_2 accumulation was detected among the inoculated seedlings of

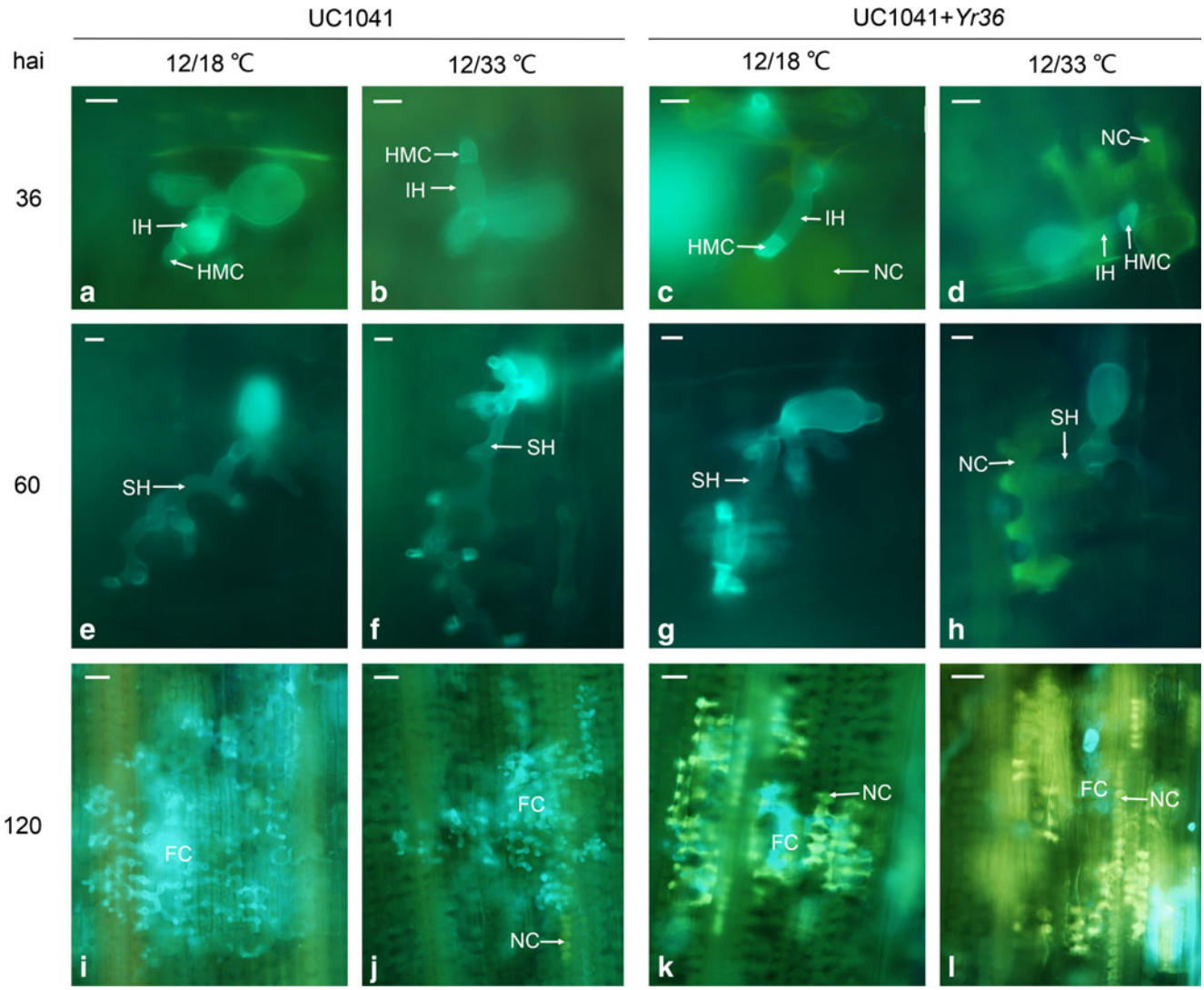

Fig. 3 Development of *Puccinia striiformis* f. sp. *tritici* (*Pst*) and host necrosis of mesophyll cells in seedling leaves of wheat lines UC1041 and UC1041+*Yr36* inoculated with race CYR29 after 36 h. **a**–**d** *Pst* primary infection hyphae expanded for differentiation and hypersensitive response (HR) of mesophyll cells in contact with secondary hyphae was observed in UC1041+*Yr36* at 36 h after inoculation; **e**–**h** secondary hyphae of *Pst* were extended in the leaves and HR of mesophyll cells adjacent to secondary hyphae was observed in UC1041+*Yr36* under high temperature; **i** HR in mesophyll cells adjacent to intercellular hyphae and neighboring cells was not observed. **j** Small amount of HR in mesophyll cells adjacent to intercellular hyphae and neighboring cells were observed. **k**, **l** The fungal colonies were surrounded by necrotic mesophyll cells in penetration sites of UC1041+*Yr36* at high temperatures. *Bars*=10 μm for **a**–**h**, *bars*=40 μm for **i**–**l**. *IH* infection hypha, *HMC* haustorial mother cell, *SH* secondary hyphae, *FC* fungal colonies, *NC* necrotic cell

UC1041 and UC1041+*Yr36* at different temperatures. DAB staining was observed at more than 80 % of the penetration sites at 18, 24, and 36 hai (Fig. 9a), indicating that UC1041+*Yr36* and UC1041 had strong reactions to *Pst* penetration. From 18 to 168 hai, the H_2O_2 burst in the infected leaves of UC1041+*Yr36* had a similar trend at different temperature treatments except 60 hai (Fig. 9a). The H_2O_2 burst in the UC1041+*Yr36* plants was decreased to a low level at the LT cycle at 60 hai, whereas the H_2O_2 burst was steadily increased at the HT cycle from 48 to 72 hai. The H_2O_2 burst in the

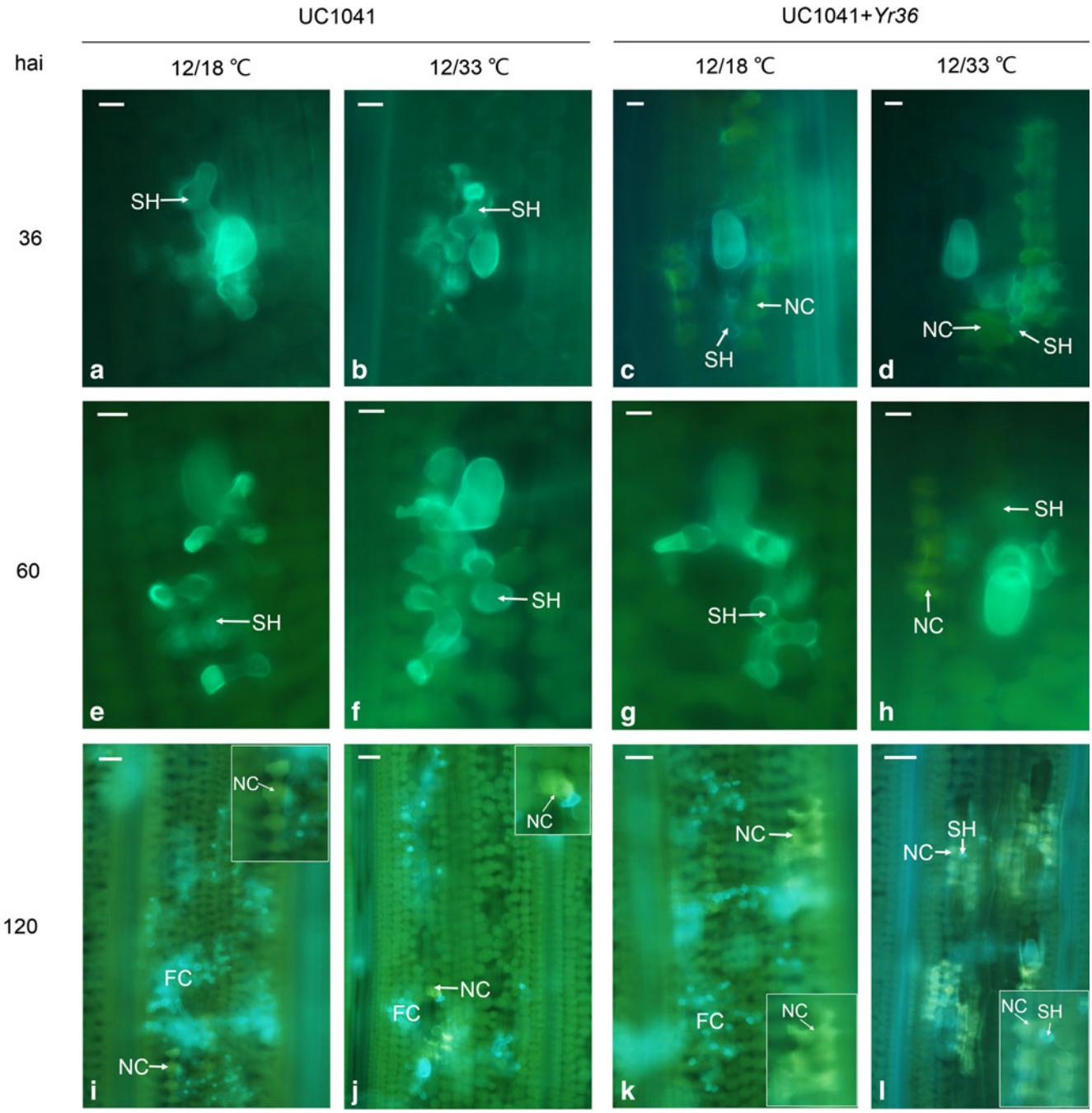

Fig. 4 Development of *Puccinia striiformis* f. sp. *tritici* (*Pst*) and host necrosis of mesophyll cells in the leaves of adult plants of UC1041 and UC1041+*Yr36* inoculated with race CYR29 after 36 h. **a**–**d** Primary hyphae were differentiated into secondary hyphae at the penetration site and hypersensitive response (HR) in mesophyll cells contacting with secondary hyphae was observed in UC1041+*Yr36*; **e**–**h** secondary hyphae of *Pst* were extended in the leaves and HR of mesophyll cells adjacent to secondary hyphae was observed in UC1041+*Yr36* under high temperature; **i**–**k** small amount of HR in mesophyll cells adjacent to intercellular hyphae and neighboring cells were observed; **l** the fungal colonies are surrounded by necrotic mesophyll cells in penetration sites of UC1041+*Yr36*. *Bars*=10 μm for **a**–**h**, *bars*=40 μm for **i**–**l**. *SH* secondary hyphae, *FC* fungal colonies, *NC* necrotic cell

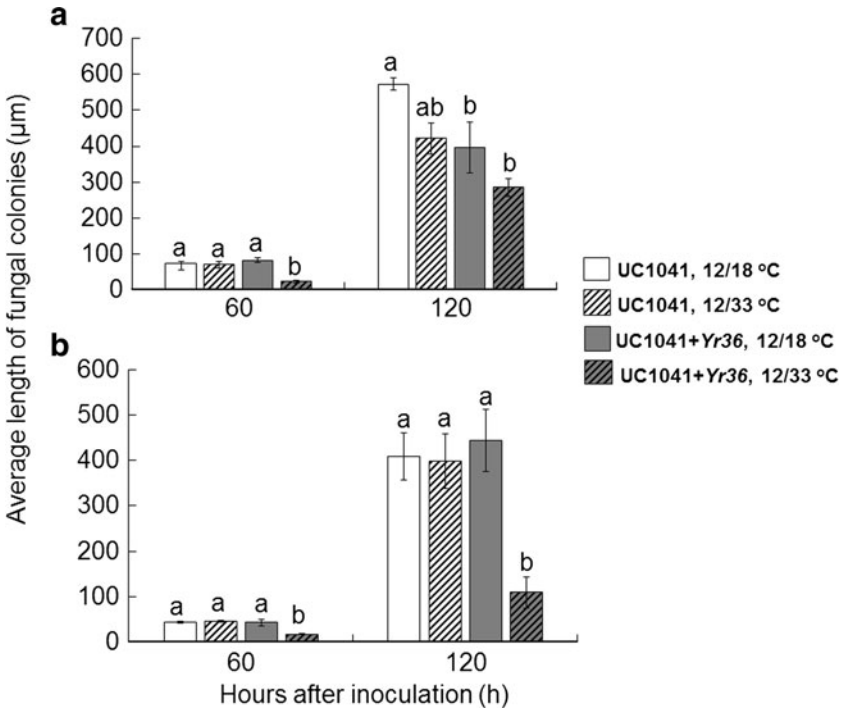

Fig. 5 Linear length of the fungal colonies parallel to the length of the leaves in plants of UC1041 and UC1041+*Yr36* at seedling (**a**) and adult-plant (**b**) stages after inoculation with *Puccinia striiformis* f. sp. *tritici.* On average, 30–50 colonies in three leaves per line at each time point were measured. *Means with the same letter* are not significantly different at $P=0.05$ according to Duncan's multiple range test. Treatments with low temperatures are indicated by *solid colors* and high temperatures by *stripes*. For each treatment, the value is the mean±standard deviation

UC1041+*Yr36* plants at the HT cycle was significantly higher than other three seedling treatments at 60 hai (Fig. 9a). For the two treatments of UC1041, the H_2O_2 accumulation of the HT test also had a higher level than that of the treatment with the LT cycle at 60 hai (Fig. 9a). The percentages of penetration sites with DAB staining of the two wheat lines in the HT tests had similar trends and were decreased to about 60 % at 120 hai. After that, the percentage of UC1041+*Yr36* started increasing while that of UC1041 did not change much until 24 h later (Fig. 9a). The high-temperature treatment had an effect on the H_2O_2 accumulation in the UC1041+*Yr36* leaves at 60 hai.

In the adult-plant stage, the H_2O_2 accumulation in the UC1041+*Yr36* leaves was intense in the guard cells of penetration sites at the early penetration stages (18–24 hai), and the level of H_2O_2 was significantly higher than that in the UC1041 leaves (Fig. 9b). From 36 to 60 hai, the percentage of penetration sites with DAB in the UC1041+*Yr36* leaves at

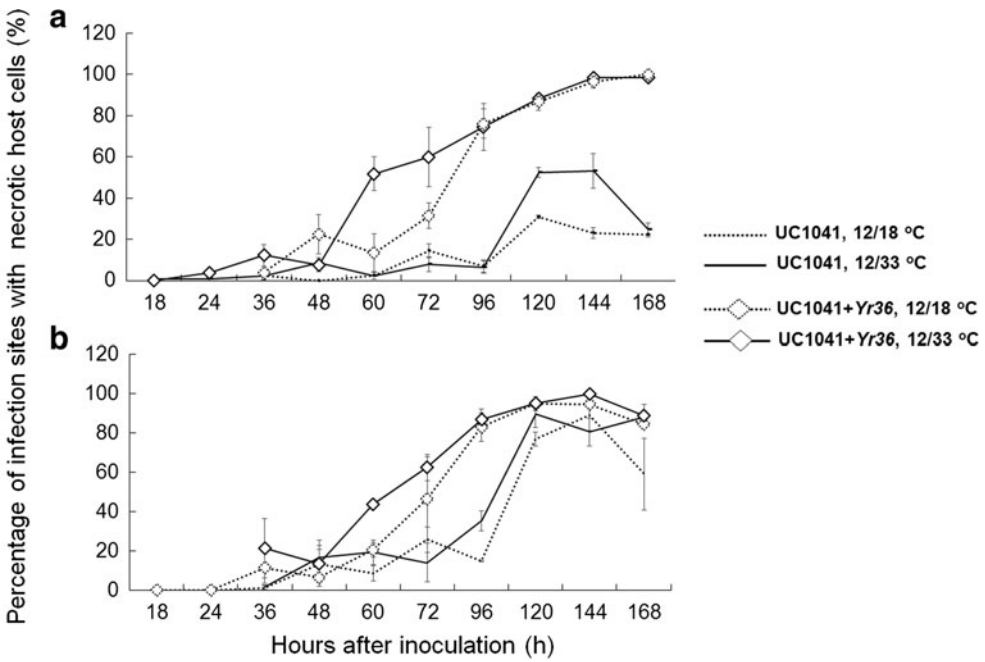

Fig. 6 Percentages of infection sites with the necrotic host cells in UC1041 and UC1041+*Yr36* leaves of plants at seedling (**a**) and adult-plant (**b**) stages after inoculation with *Puccinia striiformis* f. sp. *tritici*. For each treatment, the value is the mean±standard deviation

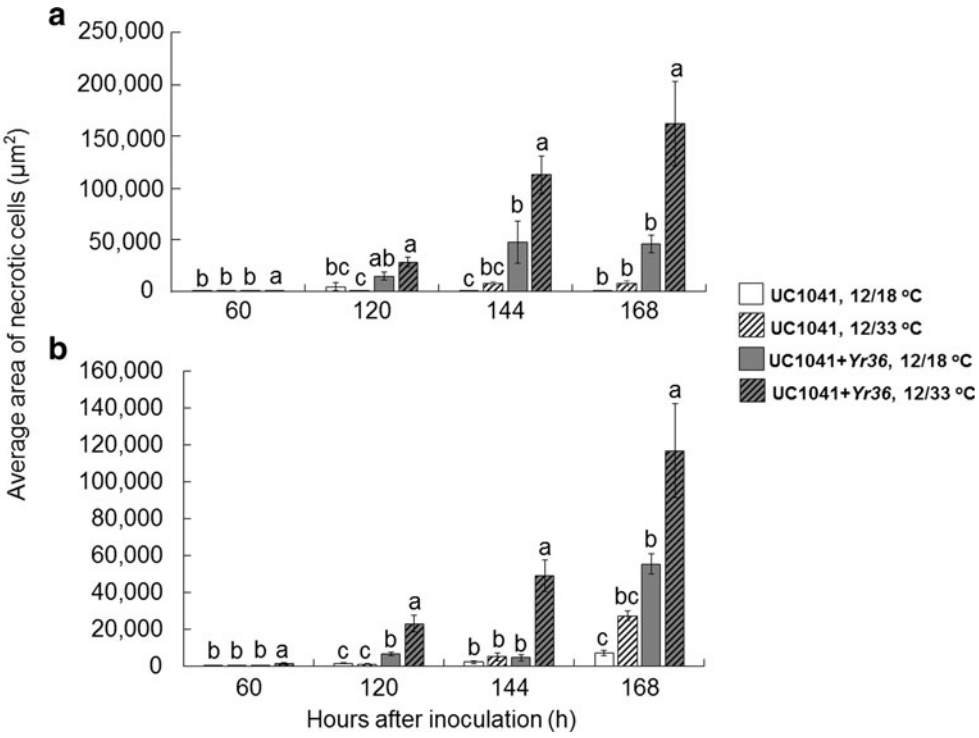

Fig. 7 Area of necrotic mesophyll cells of infection sites in the leaves of UC1041 and UC1041+*Yr36* at seedling (**a**) and adult-plant (**b**) stages after inoculation with *Puccinia striiformis* f. sp. *tritici*. On average, 30–50 microscopic fields of necrotic mesophyll cells at infection sites in three leaves per line at each time point were measured. *Means with the same letter* are not significantly different at $P=0.05$ according to Duncan's multiple range test. Treatments with low temperatures are indicated by *solid colors* and high temperatures by *stripes*. For each treatment, the value is the mean±standard deviation

HT was increased instantly, reaching 94.6 % at 60 hai (Fig. 9b). During this period, the H_2O_2 burst in the UC1041+*Yr36* plants at HT was the highest among all adult-plant treatments (Fig. 9b). The H_2O_2 burst in the UC1041+*Yr36* leaves at HT was significantly higher than that in the UC1041+*Yr36* leaves at LT and the UC1041 leaves at HT at 48 and 60 hai (Fig. 9b). Of all adult-plant treatments, the percentage remained constantly over 80 % after 60 hai (Fig. 9b). For the UC1041 plants tested at LT, the percentage of penetration sites with DAB staining was at the lowest level at 48 hai and slightly changed after 60 hai (Fig. 9b). However, the percentage in the UC1041 leaves at HT was decreased to 58.4 % at 60 hai and started to increase afterwards (Fig. 9b). At the adult-plant stage, the H_2O_2 generation in the UC1041+*Yr36* leaves was effected by *Yr36* during the periods of 18–36 and 36–60 hai at LT and HT, respectively.

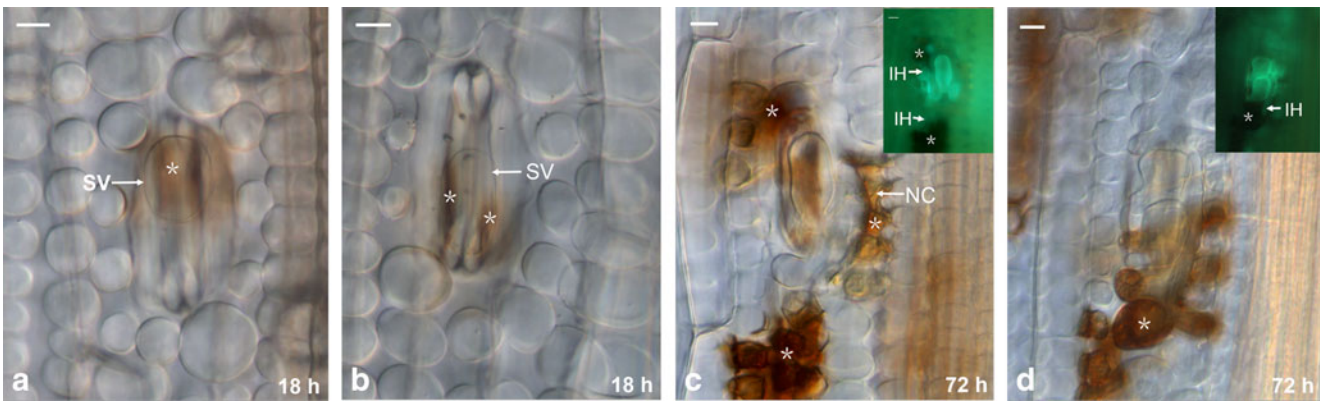

Fig. 8 Histochemical localization of H_2O_2 at interaction sites in adult plants UC1041 and UC1041+*Yr36* after inoculation with *Puccinia striiformis* f. sp. *tritici* (*Pst*). Pictures **a**–**d** were obtained using a differential interference microscope. Guard cells of UC1041 (**a**) and UC1041+*Yr36* (**b**) showing reddish-brown staining (*asterisk*) in the interaction between wheat and *Pst*. **c** Mesophyll cells of wheat UC1041 under the high-temperature (HT) cycle (12 °C at night and 33 °C during the day) in contact with an infection hypha showing intensive H_2O_2 accumulation (*asterisk*), but uneven distribution in infected cells undergoing hypersensitive response (HR). **d** Mesophyll cells of wheat UC1041+*Yr36* under the HT cycle in contact with infection hypha showing intensive H_2O_2 accumulation (*asterisk*). *Bars*=10 µm. *SV* substomatal vesicle, *IH* infection hypha, *NC* necrotic cell. The inoculated plants were placed in a dew chamber without light at 10 °C for 24 h and then divided into two groups. One group was grown in a greenhouse at the HT cycle and the other group at a low-temperature (LT) cycle (12 °C at night and 18 °C during the day)

The effect of *Yr36* on O_2^- accumulation in host cells

The O_2^- generation of few penetration sites was detected at 18 and 24 hai and remained stable and at low levels until 96 hai in the four seedling treatments. For the two temperature treatments of UC1041+*Yr36*, the percentage of penetration sites with NBT staining began increasing at 96 hai (Fig. 10a). After that, the O_2^- accumulation under the HT treatment had a sharp and steady increase (Fig. 10a). In contrast, the percentage of the LT treatment was decreased from 46.5 % at 120 hai to 35.4 % at 144 hai and then started increasing again (Fig. 10a). The percentage of penetration sites showing NBT staining in the UC1041+*Yr36* plants was increased to about 60 % under different temperature treatments at 168 hai (Fig. 10a). The first peak of O_2^- accumulation appeared at 60 hai and another peak was reached during the period of 120–144 hai for both LT and HT treatments of UC1041. Specifically, the percentage of the LT treatment started increasing after 96 hai, reached 62.4 % at 120 hai, and remained at similar level until 144 hai before decreasing (Fig. 10a). In contrast, the percentage of the HT treatment began increasing at 120 hai and peaked at 45.2 % 24 h later (Fig. 10a). For adult-plants of UC1041+*Yr36* at HT, the first peak of O_2^- generation coincided with the increase in differentiation of primary hyphae and the highest percentage of penetration sites with hypersensitive cell death (Fig. 11). The second peak of O_2^- generation coincided with the intensely extension of fungal colonies and the increase of necrotic host cells surrounding the tacked cells (Fig. 12). The O_2^- burst in the leaves infected by *Pst* was different between UC1041 and UC1041+*Yr36* at the seedling stage.

The O_2^- generation of penetration sites was detected at 18 hai at the adult-plant stage (Fig. 10b). The two peaks of the O_2^- accumulation of UC1041+*Yr36* appeared at 60 and 144 hai, while those of UC1041 appeared at 72 and 144 hai (Fig. 10b). The percentages at the two peaks of UC1041+*Yr36* at HT were the highest among the four adult-plant treatments, which were 24.1 % at 60 hai and 21.6 % at 144 hai. The percentage at the peak of UC1041+*Yr36* in the HT test was significantly higher than those of the other adult-plant treatments at 60 hai (Fig. 10b). In the UC1041 plants, the percentage was 11 % for the LT treatment and only 2.4 % for the HT treatment at 72 hai. However, the amount of O_2^- accumulation in the HT test was higher than that of LT at 144 hai. The time points to reach the peak of O_2^- accumulation and the levels were different between UC1041 and

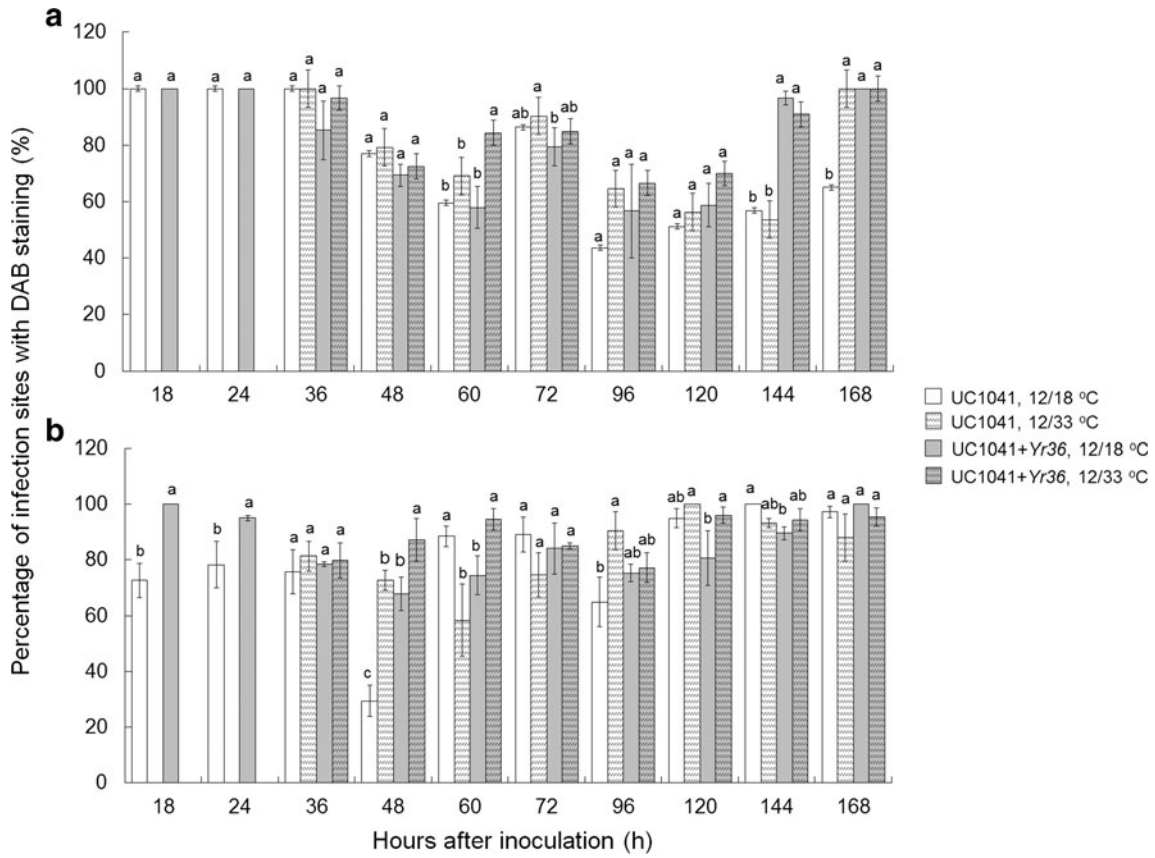

Fig. 9 Percentages of infection sites exhibiting H_2O_2 accumulation in the leaves of UC1041 and UC1041+*Yr36* at seedling and adult-plant stages after inoculation with *Puccinia striiformis* f. sp. *tritici* representing the seedling tests (**a**) and the adult-plant tests (**b**). For each treatment, the value is the mean±standard deviation. *Means with the same letter* are not significantly different at $P=0.05$ according to Duncan's multiple range test

UC1041+*Yr36*. High temperature enhanced O_2^- accumulation compared with LT in the infected leaves of UC1041+*Yr36*.

During the *Pst* infection, the level of O_2^- accumulation was lower than that of the H_2O_2 accumulation. The burst of H_2O_2 and O_2^- occurred earlier than the hypersensitive cell death reaction in the infected leaves.

Discussion

Yr36 was characterized as a gene conferring HTAP resistance as the gene-carrying wheat line UC1041+*Yr36* had an increased level of resistance in the adult-plant stage tested under a high-temperature (10–30 °C) cycle compared to seedlings tested at a low-temperature (4–20 °C) cycle (Uauy et al. 2005). Later, the gene was shown to have some effectiveness in seedlings at high temperatures (Fu et al. 2009). In the present study, we also found that the *Yr36* line was resistant to stripe rust at both seedling and adult-plant stages tested at the LT (12/18 °C) and HT (12/33 °C) cycles with the highest level of resistance detected in the HT and adult-plant test. In contrast, the susceptible control AvS was susceptible in all four-way (seedling LT, seedling HT, adult-plant LT, and adult-plant HT) tests (Chen 2013), indicating that both the LT and HT conditions were suitable for differentiating between resistant and susceptible reactions. The results were consistent with previous studies (Uauy et al. 2005; Fu et al. 2009) showing that *Yr36* is sensitive to temperatures. In addition, we found that UC1041 has some level of resistance, consistent with the report by Bryant et al. (2014) that UC1041 possesses stripe rust resistance independent of *Yr36*. Furthermore, the present study demonstrated that cell death and ROS burst are involved in the *Yr36* resistance to stripe rust.

The phenomenon of oxidative burst was first reported by Doke (1983), who demonstrated that potato tuber generated O_2^- following inoculation with an avirulent race of *Phytophthora infestans* and O_2^- generated to be involved in triggering phytoalexin synthesis and hypersensitive cell death in potato. Since then, many studies have elucidated the role of ROS in defense responses during plant-pathogen interactions

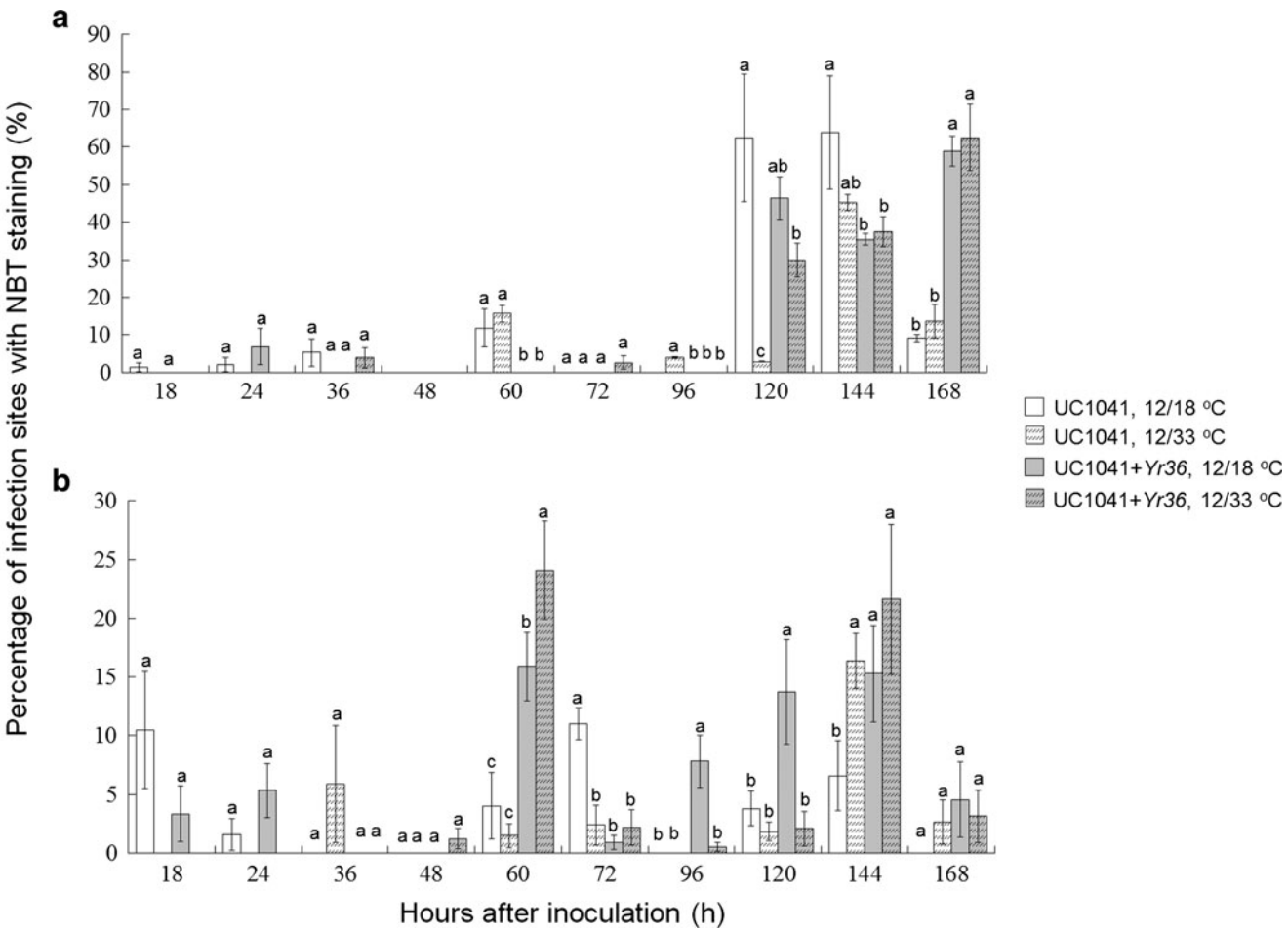

Fig. 10 Percentages of infection sites exhibiting O_2^- accumulation in the leaves of UC1041 and UC1041+*Yr36* at seedling and adult-plant stages after inoculation with *Puccinia striiformis* f. sp. *tritici* representing the seedling tests (**a**) and the adult plant tests (**a**). For each treatment, the value is the mean±standard deviation. *Means with the same letter* are not significantly different at $P=0.05$ according to Duncan's multiple range test

(Torres 2010). H_2O_2 and O_2^- are primary ROS species at the site of attempted invasion of pathogen (Apostol et al. 1989). In order to detect the accumulation of H_2O_2 and O_2^-, many kinds of methods have been developed. These methods are based on histochemical staining, cytochemical localization, fluorescence, luminescence, or electron paramagnetic resonance spectroscopy (Lehmann et al. 2014). Among them, the histochemical methods based on DAB and NBT staining were widely used for specific visualized detection of H_2O_2 and O_2^- in planta under biotic stress (Doke 1983; Thordal-Christensen et al. 1997; Rossetti and Bonatti 2001; Mellersh et al. 2002; Wang et al. 2007; Dubreuil-Maurizi et al. 2010; Kobayashi et al. 2012; Simon et al. 2013) and abiotic stress (Orozco-Cardenas and Ryan 1999; Acar et al. 2001; Romero-Puertas et al. 2004; Hu et al. 2005; Mullineaux et al. 2006; Hsu and Kao 2007; Chao et al. 2010) conditions, respectively. DAB is a substrate of peroxidase and forms a brownish polymer in the presence of H_2O_2 (Thordal-Christensen et al. 1997). NBT is yellow in color and water soluble, and it is changed to blue and water-insoluble formazan when interacting with O_2^- (Beauchamp and Fridovich 1971). There was no report on nonspecific histochemical staining of DAB and NBT for H_2O_2 and O_2^- in plant tissue.

In the present study, using DAB and NBT staining, we found that ROS accumulation in *Pst*-infected UC1041+*Yr36* leaves was enhanced during the intense extension of SH

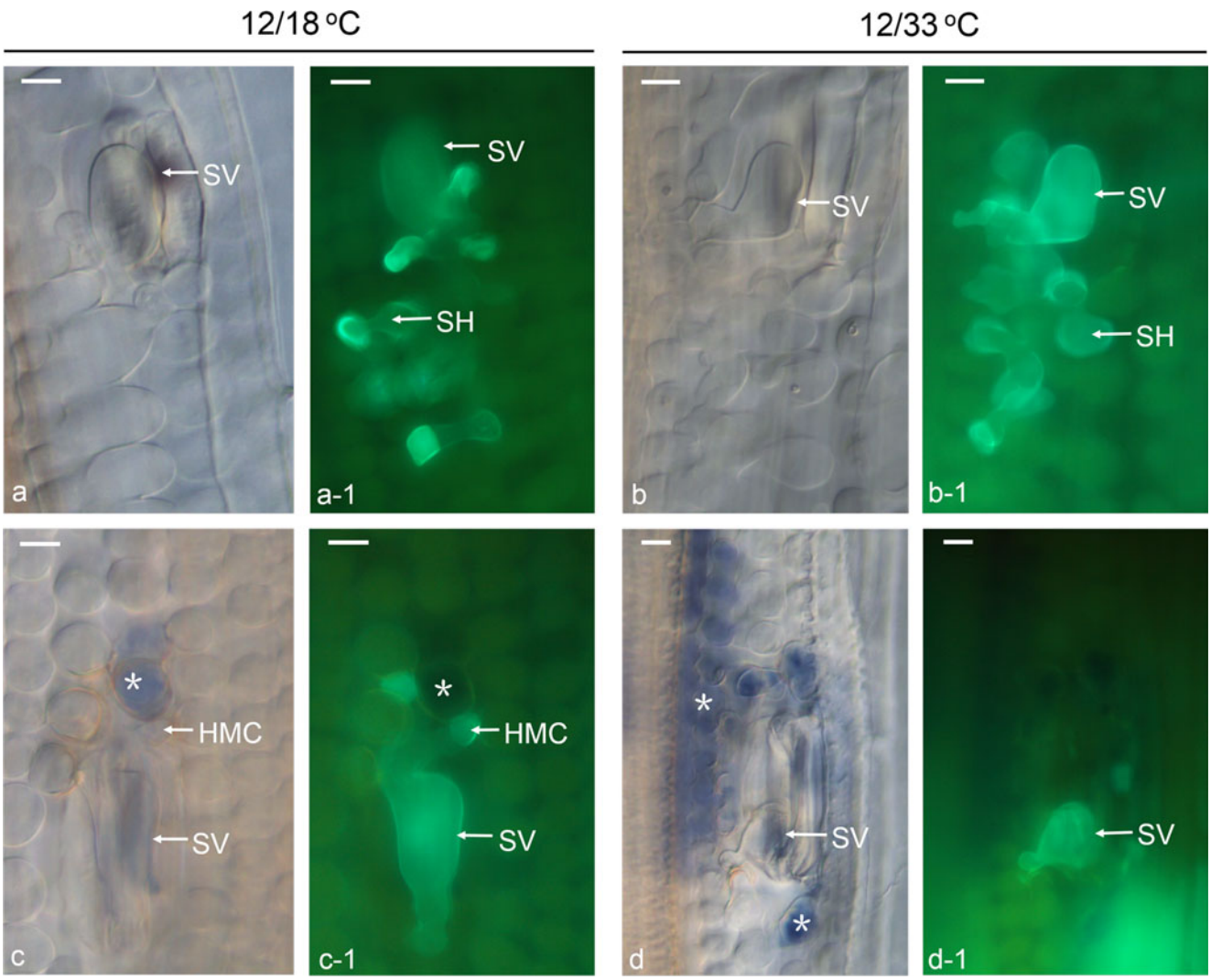

Fig. 11 Histochemical localization of O_2^- production in adult-plant leaves of UC1041 and UC1041+*Yr36* at 60 h after inoculation with *Puccinia striiformis* f. sp. *tritici* race CYR29. Pictures **a**–**d** were obtained using a differential interference microscope. **a**-*1*, **b**-*1*, **c**-*1*, and **d**-*1* were obtained from observations of **a**, **b**, **c,** and **d** under a fluorescent microscope, respectively. **a**, **b** O_2^- accumulation was not detected in the infected leaves of UC1041. **c** The mesophyll cell in contact with the haustorial mother cell showing O_2^- accumulation (*asterisk*). **d** Mesophyll cells in contact with infection hyphae showing intensive O_2^- accumulation (*asterisk*). *Bars*=10 μm. *SV* substomatal vesicle, *HMC* haustorial mother cell, *SH* secondary hyphae. For the temperature treatments, 12/18 °C means that plants were kept in a controlled greenhouse at 16 h light/8 h dark cycle and temperatures at 12 °C during the dark period and 18 °C during the light period; 12/33 °C means that temperature regime had a gradual change between a minimum of 12 °C at the middle of the dark period to a maximum of 33 °C at the middle of the light period

(60 hai) and the strong expansion of fungal colonies (144 hai) at HT. In the meantime, the cell death was increased. In addition, the H_2O_2 accumulation had significantly higher level in the *Pst*-infected adult plants of UC1041+*Yr36* than in the UC1041 plants when most SVs were differentiated into primary infection hyphae and HMC (18 and 24 hai). In other words, the ROS accumulation in the *Pst*-infected UC1041+*Yr36* leaves was increased when the pathogen needed to obtain nutrients from plant cells using haustoria for further growth.

The observed increased stain at infection sites and the surrounding *Pst* hyphae should be due to the increased H_2O_2 levels that resulted from the plant defense against *Pst* under the HT effect rather than by any temperature effect on staining. Because no stain or much low levels of stain were observed in the susceptible control (AvS) leaf tissues in the noninoculated and inoculated plants, respectively, of different growth stages at the LT and HT cycles (data not shown), the DAB and NBT staining specifically detected ROS related to plant defense. The specificity of the DAB or NBT staining was also supported by the different levels of H_2O_2 and O_2^- accumulation in the different inoculated treatments of UC1041+*Yr36* and UC1041 at different growth stages and time points during the interaction process under different temperatures. The differences were correlated well with the observed macroscopic phenotypical differences and microscopic cell death. ROS as signaling molecules are involved in coordinate plant defense to biotic stress, including the HR (Torres et al. 2006; Torres 2010; Vellosillo et al. 2010; Coll et al. 2011; Spoel and Loake

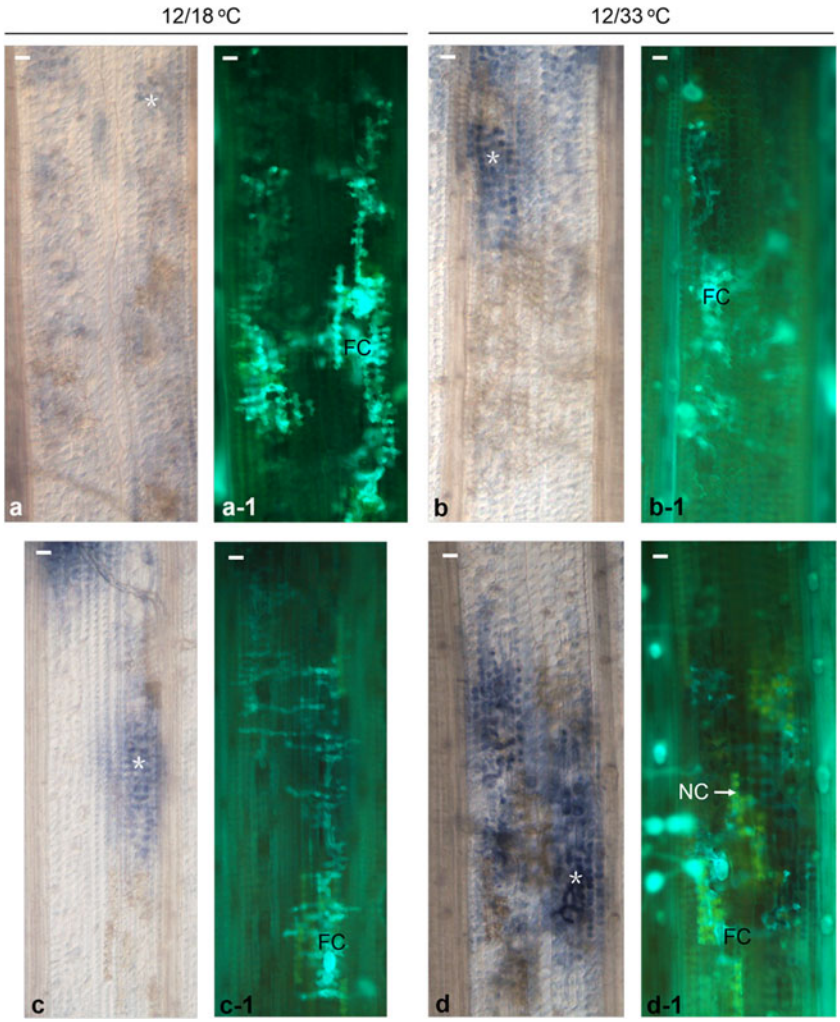

Fig. 12 Histochemical localization of O_2^- production in adult-plant leaves of UC1041 and UC1041+*Yr36* at 144 h after inoculation with *Puccinia striiformis* f. sp. *tritici* race CYR29. Pictures **a**–**d** were obtained using a differential interference microscope. **a-***1*, **b-***1*, **c-***1*, and **d-***1* were obtained from observations of **a**, **b**, **c,** and **d** under a fluorescent microscope, respectively. **a**–**c** The mesophyll cell in contact with the fungal colonies showing O_2^- accumulation (*asterisk*). **d** The mesophyll cells in contact with fungal colonies showing intensive O_2^- accumulation (*asterisk*); and living mesophyll cells around hypersensitive response (HR) cells show NBT staining (*asterisk*). *Bars*=20 μm. *FC* fungal colonies, *NC* necrotic cell. For the temperature treatments, 12/18 °C means that plants were kept in a controlled greenhouse at 16 h light/8 h dark cycle and temperatures at 12 °C during the dark period and 18 °C during the light period; 12/33 °C means that temperature regime had a gradual change between a minimum of 12 °C at the middle of the dark period to a maximum of 33 °C at the middle of the light period

2011; Bellin et al. 2012). ROS induce HR of infected cells (Levine et al. 1994; Tenhaken et al. 1995; Jabs et al. 1996; Hückelhoven et al. 1999; Bolwell et al. 2001) and ROS-induced HR can act as a defense reaction against avirulent pathogen (Delledonne et al 1998; Hückelhoven et al. 1999). Therefore, we conclude that ROS burst and HR are involved in the *Yr36* resistance to stripe rust.

The ROS level usually keeps a dynamic balance between the production and scavenging in plants of regular growth (Mittler et al. 2004). However, biotic and abiotic stresses can affect the production or scavenging system of ROS to break the balance in responding to the environmental stimulus (Apel and Hirt 2004). In the present study, the ROS accumulation in the wheat leaf tissues stimulated by *Pst* was different among the different time points. Such dynamics of ROS during the interaction of wheat-*Pst* was similar to the previous studies on other plant-pathogen interactions, such as rose-*Phytophthora* spp., tobacco-*Pseudomonas syringae*, Arabidopsis-*Fusarium oxysporum*, and Arabidopsis-*Colletotrichum lindemuthianum* (Auh and Murphy 1995; Harding and Roberts 1998; Bindschedler et al. 2006).

Yr36 encodes a WKS1 protein (Fu et al. 2009). The protein expression could be upregulated by high temperatures. Based on our observations in the present study, we hypothesize that the *Yr36* product affects the levels of ROS-producing and/or scavenging enzymes at HT, resulting in the increase of ROS, and then the ROS molecules contribute to the host cell death that consequently suppresses the *Pst* hyphal growth. Further studies are needed to test the hypothesis and understand how the gene product is involved in the increase of ROS. At some of the time points examined, ROS also had an increased level in the *Pst*-infected UC1041 plants, which might be due to the resistance of UC1041 conferred by an unknown gene independent of *Yr36* (Bryant et al. 2014).

Most of the disease resistance genes in plants cloned to date encode nucleotide-binding site leucine-rich repeat (NBS-LRR) proteins. The NBS-LRR proteins are involved in the recognition of specialized pathogen effectors by direct or indirect interactions, activating defense responses of the plants to the corresponding pathogens (DeYoung and Innes 2006). However, *Yr36* is not a NBS-LRR gene, as it encodes a kinase domain and a START domain (Fu et al. 2009). The serine-threonine kinase domain was confirmed to have kinase activity and the complete START domain was found to be essential for the *Yr36* resistance at high temperatures. The kinase encoded by *Yr36* belongs to a non-RD kinase group (Fu et al. 2009). Many non-RD kinases do not autophosphorylate the activation loop (Dardick and Ronald 2006). These kinases are either constitutively active or regulated through alternative autophosphorylation of the activation loop (Johnson et al. 1996). Dardick and Ronald (2006) found that non-RD kinases serve as pathogen recognition receptors. The START domain of such a protein in mammals plays versatile roles in intracellular lipid transport, lipid metabolism, and cell signaling events (Alpy and Tomasetto 2005). The *Yr36*-encoded WKS1 protein may have a specific mechanism to recognize and activate resistance to *Pst* at different growth stages under the influence of temperature. As *Yr36* is not a NBS-LRR gene, it could be classified into the nonrace specific and durable type of resistance genes (Chen 2013). In fact, wheat cultivars with *Yr36*, such as 'Farnum,' have been resistant for more than 10 years since widely grown in the US Pacific Northwest (XM Chen, personal communication). Because the level of resistance conferred by *Yr36* is affected by temperatures, it should be more useful if combined with genes less dependent of temperatures in wheat cultivars to provide adequate resistance to stripe rust in a wider range of environments.

Acknowledgments We thank Ms. Guorong Wei, Mr. Yingchao Chen, and the Innovation experimental group led by Shan Zhang for assisting in the greenhouse experiments. We thank Dr. Daolin Fu and Dr. Jorge Dubcovksy for the provision of seeds of near-isogenic lines UC1041 and UC1041+*Yr36*. We would like to thank Dr. Xianming Chen for critically reviewing the manuscript. We also thank Dr. Chenfang Wang for comments on this manuscript prior to submission. This research was supported by the National Major Project of Breeding for New Transgenic Organisms in China (2009ZX08009-053B) and the National Key Basic Research Program of China (2013CB127700).

Conflict of interest We declare that we do not have any commercial or associative interest that represents a conflict of interest in connection with the work submitted.

References

Acar O, Türkan I, Özdemir F (2001) Superoxide dismutase and peroxidase activities in drought sensitive and resistant barley (*Hordeum vulgate* L.) varieties. Acta Physiol Plant 23:351–356

Alpy F, Tomasetto C (2005) Give lipids a START: the StAR-related lipid transfer (START) domain in mammals. J Cell Sci 118:2791–2801

Apel K, Hirt H (2004) Reactive oxygen species: metabolism, oxidative stress, and signal transduction. Annu Rev Plant Biol 55:373–99

Apostol I, Heinstein PF, Low PS (1989) Rapid stimulation of an oxidative burst during elicitation of cultured plant cells. Plant Physiol 90:109–116

Auh CK, Murphy TM (1995) Plasma membrane redox enzyme is involved in the synthesis of O_2^- and H_2O_2 by *Phytophthora* elicitor-stimulated rose cells. Plant Physiol 107:1241–1247

Beauchamp C, Fridovich I (1971) Superoxide dismutase: improved assays and an assay applicable to acrylamide gels. Anal Biochem 44: 276–287

Bellin D, Asai S, Delledonne M, Yoshioka H (2012) Nitric oxide as a mediator for defense responses. Mol Plant Microbe Interact 26:271–277

Bindschedler LV, Dewdney J, Blee KA, Stone JM, Asai T, Plotnikov J, Denoux C, Hayes T, Gerrish C, Davies DR, Ausubel FM, Bolwell GP (2006) Peroxidase-dependent apoplastic oxidative burst in Arabidopsis required for pathogen resistance. Plant J 47:851–863

Bolwell PP, Page A, Piślewska M, Wojtaszek P (2001) Pathogenic infection and the oxidative defences in plant apoplast. Protoplasma 217: 20–32

Bozkurt TO, McGrann GRD, MacCormack R, Boyd LA, Akkaya MS (2010) Cellular and transcriptional responses of wheat during compatible and incompatible race-specific interactions with *Puccinia striiformis* f. sp. *tritici*. Mol Plant Pathol 11:625–640

Bryant RRM, McGrann GRD, Mitchell AR, Schoonbeek H, Boyd LA, Uauy C, Dorling S, Ridout CJ (2014) A change in temperature modulates defence to yellow (stripe) rust in wheat line UC1041 independently of resistance gene *Yr36*. BMC Plant Biol. doi:10.1186/1471-2229-14-10

Chao YY, Chen CY, Huang WD, Kao CH (2010) Salicylic acid-mediated hydrogen peroxide accumulation and protection against Cd toxicity in rice leaves. Plant Soil 329:327–337

Chen XM (2005) Epidemiology and control of stripe rust on wheat. Can J Plant Pathol 27:314–337

Chen XM (2013) Review article: high-temperature adult-plant resistance, key for sustainable control of stripe rust. Am J Plant Sci 4:608–627

Chen XM, Line RF (1995a) Gene action in wheat cultivars for durable high-temperature adult-plant resistance and interactions with race-specific, seedling resistance to stripe rust caused by *Puccinia striiformis*. Phytopathology 85:567–572

Chen XM, Line RF (1995b) Gene number and heritability of wheat cultivars with durable, high-temperature, adult-plant resistance and race-specific resistance to *Puccinia striiformis*. Phytopathology 85:573–578

Chen XM, Moore M, Milus EA, Long DL, Line RF, Marshall D, Jackson L (2002) Wheat stripe rust epidemics and races of *Puccinia striiformis* f. sp. *tritici* in the United States in 2000. Plant Dis 86:39–46

Chen WQ, Wu LR, Liu TG, Xu SC (2009) Race dynamics, diversity, and virulence evolution in *Puccinia striiformis* f. sp. *tritici*, the causal agent of wheat stripe rust in China from 2003 to 2007. Plant Dis 93:1093–1101

Coll NS, Epple P, Dangl JL (2011) Programmed cell death in the plant immune system. Cell Death Differ 18:1247–1256

Coram TE, Wang MN, Chen XM (2008) Transcriptome analysis of the wheat-*Puccinia striiformis* f. sp. *tritici* interaction. Mol Plant Pathol 9:157–169

Dardick C, Ronald P (2006) Plant and animal pathogen recognition receptors signal through non-RD kinases. PLoS Pathog 2:14–28

Delledonne M, Xia YJ, Dixon RA, Lamb C (1998) Nitric oxide functions as a signal in plant disease resistance. Nature 394:585–588

DeYoung BJ, Innes RW (2006) Plant NBS-LRR proteins in pathogen sensing and host defense. Nat Immunol 7:1243–1249

Dodds PN, Rathjen JP (2010) Plant immunity: towards an integrated view of plant-pathogen interactions. Nat Rev Genet 11:539–548

Doke N (1983) Involvement of superoxide anion generation in the hypersensitive response of potato tuber tissues to infection with an incompatible race of *Phytophthora infestans* and to the hyphal wall components. Physiol Plant Pathol 23:345–57

Dubreuil-Maurizi C, Trouvelot S, Frettinger P, Pugin A, Wendehenne D, Poinssot B (2010) β-Aminobutyric acid primes an NADPH oxidase-dependent reactive oxygen species production during grapevine-triggered immunity. Mol Plant Microbe Interact 23:1012–1021

Fu DL, Uauy C, Distelfeld A, Blechl A, Epstein L, Chen XM, Sela H, Fahima T, Dubcovsky J (2009) A kinase-START gene confers temperature-dependent resistance to wheat stripe rust. Science 323:1357–1360

Harding SA, Roberts DM (1998) Incompatible pathogen infection results in enhanced reactive oxygen and cell death responses in transgenic tobacco expressing a hyperactive mutant calmodulin. Planta 206:253–258

Hsu YT, Kao CH (2007) Heat shock-mediated H_2O_2 accumulation and protection against Cd toxicity in rice seedlings. Plant Soil 300:137–147

Hu XL, Jiang MY, Zhang AY, Lu J (2005) Abscisic acid-induced apoplastic H_2O_2 accumulation up-regulates the activities of chloroplastic and cytosolic antioxidant enzymes in maize leaves. Planta 223:57–68

Hückelhoven R, Fodor J, Preis C, Kogel KH (1999) Hypersensitive cell death and papilla formation in barley attacked by the powdery mildew fungus are associated with hydrogen peroxide but not with salicylic acid accumulation. Plant Physiol 119:1251–1260

Jabs T, Dietrich RA, Dangl JL (1996) Initiation of runaway cell death in an *Arabidopsis* mutant by extracellular superoxide. Science 273:1853–6

Johnson LN, Nobel MEM, Owen DJ (1996) Active and inactive protein kinases: structural basis for regulation. Cell 85:149–158

Kang ZS, Shang HS, Li ZQ (1993) Fluorescence staining techniques of wheat tissue infected by stripe rust (in Chinese). Acta Phytophy Sin 2:27

Kang ZS, Wang Y, Huang LL, Wei GR, Zhao J (2003) Histology and ultrastructure of incompatible combination between *Puccinia striiformis* and wheat cultivars with low reaction type resistance. Agric Sci China 2:1102–1113

Kobayashi M, Yoshioka M, Asai S, Nomura H, Kuchimura K, Mori H, Doke N, Yoshioka H (2012) StCDPK5 confers resistance to late blight pathogen but increases susceptibility to early blight pathogen in potato via reactive oxygen species burst. New Phytol 196:223–237

Lamb C, Dixon RA (1997) The oxidative burst in plant disease resistance. Annu Rev Plant Biol 48:251–275

Lehmann S, Serrano M, L'Haridon F, Tjamos SE, Metraux JP (2014) Reactive oxygen species and plant resistance to fungal pathogens. Phytochemistry 112:54–62

Levine A, Tenhaken R, Dixon R, Lamb C (1994) H_2O_2 from the oxidative burst orchestrates the plant hypersensitive disease resistance response. Cell 79:583–93

Lin F, Chen XM (2007) Genetics and molecular mapping of genes for race-specific all-stage resistance and non-race specific high-temperature adult-plant resistance to stripe rust in spring wheat cultivar Alpowa. Theor Appl Genet 114:1277–1287

Lin F, Chen XM (2009) Quantitative trait loci for non-race specific, high-temperature adult-plant resistance to stripe rust in wheat cultivar express. Theor Appl Genet 118:631–642

Line RF (2002) Stripe rust of wheat and barley in North America: a retrospective historical review. Annu Rev Phytopathol 40:75–118

Line RF, Chen XM (1995) Success in breeding for and managing durable resistance to wheat rusts. Plant Dis 79:1254–1255

Line RF, Qayoum A (1992) Virulence, aggressiveness, evolution, and distribution of races of *Puccinia striiformis* (the cause of stripe rust of wheat) in North America, 1968–87. US Dept. of Agriculture, Agricultural Research Service, Technical Bulletin 1788

Liu N, Lin ZF (2014) Reaction oxygen species and relative enzyme activities in the development of aerial roots of Chinese banyan (*Ficus microcarpa*). J Plant Growth Regul 33:160–168

Mellersh DG, Foulds IV, Higgins VJ, Heath MC (2002) H_2O_2 plays different roles in determining penetration failure in three diverse plant-fungal interactions. Plant J 29:257–268

Milus EA, Line RF (1986a) Number of genes controlling high temperature adult-plant resistance to stripe rust in wheat. Phytopathology 76:93–96

Milus EA, Line RF (1986b) Gene action for inheritance of durable, high-temperature, adult-plant resistance to stripe rust in wheat. Phytopathology 76:435–441

Mittler R, Vanderauwera S, Gollery M, Breusegem FV (2004) Reactive oxygen gene network of plants. Trends Plant Sci 9:490–497

Mullineaux PM, Karpinski S, Baker NR (2006) Spatial dependence for hydrogen peroxide-directed signaling in light-stressed plants. Plant Physiol 141:346–350

Orozco-Cardenas M, Ryan C (1999) Hydrogen peroxide is generated systemically in plant leaves by wounding and systemin via the octadecanoid pathway. Proc Natl Acad Sci U S A 96:6553–6557

Qayoum A, Line RF (1985) High-temperature, adult-plant resistance to stripe rust of wheat. Phytopathology 75:1121–1125

Romero-Puertas MC, Rodríguez-Serrano M, Corpas FJ, Gómez M, Del Río LA, Sandalio LM (2004) Cadmium-induced subcellular accumulation of O_2^- and H_2O_2 in pea leaves. Plant Cell Environ 27: 1122–1134

Rossetti S, Bonatti PM (2001) In situ histochemical monitoring of ozone- and TMV-induced reactive oxygen species in tobacco leaves. Plant Physiol Biochem 39:433–442

Rubiales D, Niks RE (1995) Characterization of *Lr34*, a major gene conferring nonhypersensitive resistance to wheat leaf rust. Plant Dis 79:1208–1212

Segovia V, Hubbard A, Craze M, Bowedn S, Wallington E, Bryant R, Greenland A, Bayles R, Uauy C (2014) *Yr36* confers partial resistance at temperatures below 18°C to U.K. isolates of *Puccinia striiformis*. Phytopathology 104:871–878

Simon UK, Polanschütz LM, Koffler BE, Zechmann B (2013) High resolution imaging of temporal and spatial changes of subcellular ascorbate, glutathione and H_2O_2 distribution during *Botrytis cinerea* infection in Arabidopsis. PLoS One 8, e65811

Singh RP (1992) Genetic association of leaf rust resistance gene *Lr34* with adult plant resistance to stripe rust in bread wheat. Phytopathology 82:835–838

Spoel SH, Loake GJ (2011) Redox-based protein modifications: the missing link in plant immune signaling. Curr Opin Plant Biol 14: 358–364

Tenhaken R, Levine A, Brisson LF, Dixon RA, Lamb C (1995) Function of the oxidative burst in hypersensitive disease resistance. Proc Natl Acad Sci U S A 92:4158–4163

Thordal-Christensen H, Zhang Z, Wei YD, Collinge DB (1997) Subcellular localization of H_2O_2 in plants. H_2O_2 accumulation in papillae and hypersensitive response during the barley-powdery mildew interaction. Plant J 11:1187–94

Torres MA (2010) ROS in biotic interactions. Physiol Plant 138:414–429

Torres MA, Jones JDG, Dangl JL (2006) Reactive oxygen species signaling in response to pathogens. Plant Physiol 41:373–378

Uauy C, Brevis JC, Chen XM, Khan I, Jackson L, Chicaiza O, Distelfeld A, Fahima T, Dubcovsky J (2005) High-temperature adult-plant (HTAP) stripe rust resistance gene *Yr36* from *Triticum turgidums* spp. *dicoccoidesis* closely linked to the grain protein content locus *Gpc-B1*. Theor Appl Genet 112:97–105

Vellosillo T, Vicente J, Kulasekaran S, Hamberg M, Castresana C (2010) Emerging complexity in reactive oxygen species production and signaling during the response of plants to pathogens. Plant Physiol 154:444–448

Wan AM, Zhao ZH, Chen XM, He ZH, Jin SL, Jia QZ, Yao G, Yang JX, Wang BT, Li GB, Bi YQ, Yuan ZY (2004) Wheat stripe rust epidemic and virulence of *Puccinia striiformis* f. sp. *tritici* in China in 2002. Plant Dis 88:896–904

Wang CF, Huang LL, Buchenauer H, Han QM, Zhang HC, Kang ZS (2007) Histochemical studies of the accumulation of reactive oxygen species (O_2^- and H_2O_2) in the incompatible and compatible interaction of wheat-*Puccinia striiformis* f. sp. *tritici*. Physiol Mol Plant Pathol 71:230–239

Wellings CR (2011) Global status of stripe rust: a review of historical and current threats. Euphytica 179:129–141

William HM, Singh RP, Huerta-Espino J, Ortiz-Islas S, Hoisington D (2003) Molecular marker mapping of leaf rust resistance gene *Lr46* and its association with stripe rust resistance gene *Yr29* in wheat. Phytopathology 93:153–159

Zhang HC, Wang CF, Cheng YL, Chen XM, Han QM, Huang LL, Wei GR, Kang ZS (2012) Histological and cytological characterization of adult plant resistance to wheat stripe rust. Plant Cell Rep 31: 2121–37